

Rapid Penumbra Decay in Active Region NOAA 9026 Associated with An X2.3 Flare

Na Deng, Chang Liu, Guo Yang, Haimin Wang, and Carsten Denker

*New Jersey Institute of Technology, Physics Department, Center for Solar-Terrestrial
Research,*

323 Martin Luther King Jr Blvd, Newark, NJ 07102-1982

nd7@njit.edu

ABSTRACT

We present observations of rapid penumbral decay associated with a major flare activity in solar Active Region NOAA 9026 on 2000 June 6. Within 1.5 hours, an X2.3 flare accompanied by an 11-degree long filament eruption and a full-halo Coronal Mass Ejection (CME) originated near the neutral line of a large δ -spot region, which was associated with significant changes in white-light structure and magnetic field topology: an increase of Moving Magnetic Features (MMFs), flux emergence and cancellation, and in particular the rapid disappearance of two penumbral segments located in opposite polarity regions on the north and south side of the δ -spot. The rapid penumbral decay is believed to be the result of magnetic field topology change that was caused by rapid magnetic reconnection during the flare rather than part of overall long-term evolution. We present a possible explanation of this event using “magnetic breakout” model for solar flares considering its complex multipolar δ configuration and associated filament eruption and CME, i.e., previously closed magnetic field lines opened up and reconnected at a null point above the neutral line of this δ -spot. The magnetic breakout caused an energy release from a highly sheared magnetic field in the umbrae and a transition of the magnetic arcades from low-lying to high-lying, which led to an increase of the inclination angle of the magnetic field lines in the peripheral penumbrae, i.e., the magnetic field turned from more inclined to more vertical and turned toward the inner umbrae. Once the magnetic field in the penumbrae was vertical enough, the Evershed flow ceased, the manifestation of which in white light structure is the disappearance of peripheral penumbrae. We also discuss other possible flare models for this event and compare them in several observational features. The present observations provide further evidence that highly energetic events have a distinct associated photospheric magnetic

field signature and support the findings of recent analysis of photospheric line-of-sight magnetograms from the Big Bear Solar Observatory (BBSO) and the Michelson Doppler Imager (MDI) on board the Solar and Heliospheric Observatory (SOHO) that show rapid and permanent changes of photospheric magnetic fields associated with flares.

Subject headings: Sun: activity — Sun: magnetic fields — Sun: coronal mass ejections (CMEs) — Sun: flares — sunspots

1. INTRODUCTION

For many decades, solar physicists have been looking for flare-related changes in the photospheric magnetic field, which would provide some information as to how an active region stores and releases its energy. However, the evolution of photospheric magnetic fields before, during, and after solar flares is still not well understood and the results have not been conclusive. For example, some authors reported a decrease in the strength of the magnetic field after, and presumably associated with, solar flares (Severny 1964; Zvereva & Severny 1970; Moore et al. 1984; Kosovichev & Zharkova 1999, 2001), some others argued that the changes are consistent with a general trend in the evolution of the magnetic fields of active regions (see Sakurai & Hiei 1996 for a review). Chen et al. (1994) studied more than 20 M-class flares and determined that there was essentially no apparent change in magnetic fields associated with the flares. The results from studies conducted at the Marshall Space Flight Center (Ambastha, Hagyard, & West 1993; Hagyard, Start, & Venkatakrisnan 1999) showed inconclusive results. The morphology of the photospheric magnetic field of an active region may or may not change as the result of a solar flare. Several very recent studies based on newly developed high spacial and temporal resolution ground and space observations provide some new exciting results related to this subject. Kosovichev & Zharkova (2001) studied high-resolution Michelson Doppler Imager (MDI) magnetogram data for the 2000 July 14 “Bastille Day Flare” and found both a permanent decrease in magnetic flux and a short-term magnetic transient. Spirock et al. (2002) found that the magnetic flux of the leading polarity increased after an X20 flare, while there was no obvious change in the magnetic flux of the following polarity. Wang et al. (2002b) found that unbalanced, rapid, and permanent flux increase might be a common property of major solar flares. Wang et al. (2004b) and Yurchyshyn et al. (2004) described the appearance of unbalanced magnetic flux that is associated with flares. Other than looking for flare-related large-scale magnetic flux change in active regions, in recent three years, we started to pay attention to the correlation between local small-scale changes of white-light structure in complex sunspots and major

flares (Wang et al. 2002a, 2004a; Liu et al. 2005). In order to thoroughly understand the correlation of magnetic flux change with energetic solar flares, more precise observations need to be done and a conclusive model need to be established. However, accurate measurements of sunspot magnetic fields can only be achieved by high-resolution two-dimensional spectropolarimetry instead of nowadays being used filter-based magnetograph systems that are not well suited for measurements of strong magnetic fields in the sunspot umbrae because of Zeeman saturation.

Antiochos (1998) and Antiochos, DeVore, & Klimchuk (1999) proposed one possible mechanism named “magnetic breakout” model for CMEs and eruptive flares that can interpret the CME and flare related magnetic field changes, in which the multipolarity of the photospheric magnetic fields plays a crucial role. In the multipolar topologies, reconnection between a sheared arcade and neighboring flux systems triggers the eruption, i.e., reconnection removes the unshaped field above the low-lying, sheared core flux near the neutral line, thereby allowing this core flux to burst open. Aulanier et al. (2000) studied an M-class flare that was accompanied by a CME and occurred in a δ -sunspot region. They found evidences supporting the “magnetic breakout” process for triggering the eruptive flare and concluded that the basic idea proposed for the breakout model is that reconnection at a null point above a sheared neutral line removes flux that tends to hold down the sheared low-lying field and thereby allows the sheared field to erupt explosively outward.

Even though the aforementioned studies and the present analysis focus on highly energetic events, we are confident that smaller events in the lower M- and C-class range will show a similar signature when observed with sufficient spatial and temporal resolution, e.g., Denker and Wang (1998) presented speckle reconstructed, diffraction limited observations of a small δ -spot, where strong proper motion of magnetic features led to a C-class flare with properties similar to major flares (Wang et al. 1991).

2. OBSERVATIONS

On 2000 June 6, GOES recorded an X2.3 flare started at 14:58 UT, peaked at around 15:25 UT and decayed slowly afterward in a δ -sunspot located at N20E18 in solar Active Region NOAA 9026. The X2.3 flare was accompanied by an 11-degree long filament eruption and a full-halo CME.

We first study the evolution of the δ -sunspot structure and find two penumbral segments at the periphery of the spot decayed rapidly and permanently within 1.5 hours associated with the X2.3 flare. These observations are quite apparent in a movie of white-light images

obtained in broadband white-light roughly centered at 5000 \AA from the Transition Region and Coronal Explorer (TRACE). The typical cadence is less than a minute and the spatial resolution is about $1''$, which make these data ideally suited for high-resolution studies of active regions (Handy et al. 1999). Unfortunately, there were only four white-light images during the time range from 14:54 UT to 16:14 UT on 2000 June 6 that covered the flare period, which can only give the association of penumbra decay with the flare within 1.5 hours.

Then, we study the line-of-sight magnetograms from MDI to investigate the photospheric magnetic field evolution. We find that the magnetic flux in the decaying penumbral regions experienced a rapid and permanent change associated with the X2.3 flare. MDI provides full-disk longitudinal magnetograms with a cadence of one minute and spatial resolution of about $4''$. The magnetograms are obtained by scanning five wavelength settings covering the Ni I 6768 \AA line. A detailed description of MDI observation and data reduction is given in Scherrer et al. (1995).

In order to study the filament eruption associated with the flare, we use high-resolution $H\alpha$ full-disk images obtained at BBSO (Denker et al. 1998). The $H\alpha$ images have 2032×2032 pixels, the cadence is one image every minute, and the spatial resolution is about $2''$. We correct the $H\alpha$ raw data by subtracting a dark frame and applying a flat-field frame. In addition, we subtract a limb darkening function to enhance the image contrast.

3. RESULTS

Studying dynamic phenomena on small scales has the potential to shed more light onto global phenomena that we frequently encounter in the context of space weather, e.g., flares, filament eruptions, and CMEs. In the present study, all three phenomena occur associated with rapid and permanent changes of white-light structure and photospheric magnetic fields in a δ -sunspot.

In Figures 1 and 2, we illustrate the evolution of NOAA 9026 from about 14:24 UT to 16:46 UT in TRACE white-light images and MDI line-of-sight magnetograms. The X2.3 flare peaked at around 15:25 UT within this time range. The penumbrae, in two regions outlined by boxes 1 and 2, partially disappeared within 1.5 hours associated with the X2.3 flare. Meanwhile, the central umbra region outlined by box 3 strengthened related to the flare and the penumbral decay. This event also produced a Type II radio burst (1189 km/s), a Type IV radio burst, an 11-degree long filament eruption, and a full-halo CME. Figure 3 shows the location of the 11-degree long filament eruption in a detailed view of BBSO full

disk H α images.

By examining movies of intensity maps and magnetograms, the most straightforward way to study the evolution of sunspot structure and magnetic fields, we find that the δ -spot in NOAA 9026 consists of four major and several minor umbral cores, which are separated by light-bridges and surrounded by complex penumbrae. The dominant magnetic neutral line is aligned with one of the light-bridges and splits the δ -spot into a northern hemisphere of positive polarity and a southern hemisphere of negative polarity. The whole δ -spot is surrounded by a ring of small sunspots and pores with an average distance from the δ -spot penumbrae of about 20'' to 40''. These small sunspots are associated with Moving Magnetic Features (MMFs), especially near the northern penumbra. During the flare the number of MMFs near the northern part of the penumbra is increasing. Most noticeably three to four distinct negative polarity magnetic features denoted by “5” in Figure 2 appear and become stronger during the period from about 14:00 UT to 17:30 UT even though there are indications that there is continuous cancellation with positive polarity features. All these negative polarity magnetic features show strong motions radially outward but become stationary once they reach the outer ring of small sunspots and pores. The flux emergence scenario in the southern hemisphere is quite different. Here, a large, isolated positive polarity magnetic feature denoted by “4” in Figure 2 is strengthening while propagating toward the west. We do not find any evidence for flux cancellation in this region. In both cases, however, localized emergence and strengthening of opposite polarity flux is involved in the flare and the subsequent disappearance of the penumbrae.

The X2.3 event is a two ribbon flare originating at the neutral line of the δ -spot, where strong gradients of the magnetic field and strongly sheared horizontal magnetic fields tend to initiate flares (Wang et al. 1994). Even before the flare started, we could observe a sporadically appearing, well defined point-like brightening moving along the neutral line at a velocity of about 0.5 km/s or less. This brightening is located within a light-bridge, i.e., the location where the southern umbral cores begin to fragment. The bright channel in the eastern part of the southern umbra is co-spatial with the initial flare line of the X2.3 flare. The two ribbons of the X2.3 flare separate at a speed of about 20 km s⁻¹ with a maximum velocity of about 30 km s⁻¹ at the initiation of the flare. Subsequently, the ribbons decelerate and the final velocity is about 15 km s⁻¹ before the flare fades away in the TRACE white-light images.

In this paper, the normalized intensity is defined as the average intensity of a certain region outlined by boxes 1, 2, and 3 in Figure 1 divided by the photospheric intensity outside the sunspot in a quiet sun region that is located at the upper-right corner of the field-of-view (FOV) of Figure 1. An intensity of 1.0 means that the region is free of sunspots. A

smaller intensity value represents a larger and/or darker sunspot in the area. In Figure 4, the intensities in areas A1 and A2 have a rapid, 4-5% increase within 1.5 hours associated with the X2.3 flare, which represents the rapid penumbral decay in these two regions, while the intensity in central umbral area A3 has a rapid, 8% decrease correlated with the flare and the penumbral decay. We excluded four data points during the flare in order to avoid the influence of the bright flare ribbons that may provide false intensity information when they moved across the selected regions. We do not find any noticeable change of the average intensity in other small sunspots outside this δ -sunspot region before and after the flare. So we deduce that the penumbral decay and umbral darkening are not related to image quality, but are really associated with the flare.

From Figure 5, we conclude that the magnetic flux decreases rapidly by 17% in A1 and is well correlated with the X2.3 flare. In A2, the magnetic flux decreases gradually instead of rapidly. Since A2 was associated with fast MMFs, the large velocity of fast MMFs may introduce some errors into the measurement of the line-of-sight magnetic field. Therefore, we do not see rapid flux decrease in A2 associated with the flare. Meanwhile, both the negative and positive magnetic fluxes in the central umbral area A3 increase by 4-7% after the flare. We notice that the flare response of the Ni line used for the MDI observations causes temporary flux dips in about 30 minutes during the flare. However, the flare emission cannot cause a permanent change after the flare. Therefore, the flux change during a long time period shown in Figure 5 is not due to the transient flare emission but relates to a real photospheric magnetic field change associated with the flare.

4. SUMMARY AND DISCUSSION

We showed the rapid decay of two sunspot penumbrae and the strengthening of the central umbrae within 1.5 hours associated with an X2.3 flare in a δ -sunspot.

A natural question arises: Is the rapid penumbral decay and central umbra darkening a coincidental phenomenon involved in the decay phase of sunspot or really closely related to the flare? Kurokawa, Wang, & Ishii (2002) studied the same flare-productive active region NOAA 9026 for its long-term evolution and found drastic changes in the δ -type sunspot configuration started several hours before the big flares of 2000 June 6. In particular they reported the catastrophic decay of the central umbrae from 10:00 UT of June 6 to 16:00 UT of June 7. They constructed a schematic model of an emerging twisted flux rope to explain these drastic evolution based on magnetic flux change in whole active region and evolution of umbrae. However, they did not mention the penumbral decay and umbral darkening phenomenon. There was no penumbra represented in their cartoon. We should distinguish

between the flare-related rapid changes (penumbral decay and central umbral darkening) in the present paper and the long-term evolution (umbral decay) in Kurokawa, Wang, & Ishii (2002). Since the long-term change is total flux change in whole active region involved in overall evolution, while flare-related change is local small-patch flux change caused by short-term magnetic reconnection. However, it is a very challenging topic to combine flare-related impulsive change and long-term evolution of active region to see what role the solar flare plays in sunspot's overall evolution (Wang et al. 2005).

Two additional papers reported the flare-related short-term penumbral decay in more flare events that occurred in other active regions, which proves that this kind of phenomenon can not be coincidental. Wang et al. (2004a) clearly showed the penumbral decay and central umbral darkening associated with three X-class flares by using the white-light difference images. They provided the following interpretation: magnetic fields turned from more inclined to more vertical after flares, which cause outside penumbrae to decay and central umbrae to strengthen. However, the light curves and physical model are not included in that paper. Liu et al. (2005) made a preliminary statistical study of rapid change of δ spot structure associated with seven major flares. They proposed a reconnection picture in which the two components of a δ spot become strongly connected after the flare.

We believe the essential reason for penumbral decay and umbral darkening phenomenon is that the magnetic field lines in peripheral penumbrae turned from more inclined to more vertical and turned toward central umbrae caused by magnetic reconnection during the flare. Once the inclination angle (the angle between magnetic field lines and the local horizon) is larger than 45° , Evershed flow will cease, the continuum-intensity signature of which is the disappearance of the associated penumbrae (Leka and Skumanich 1998).

In this paper, we try to pursue a flare model to interpret the observed flare-related rapid changes in the multipolar photospheric magnetic configuration. The emerging twisted flux rope model presented in Kurokawa, Wang, & Ishii (2002) suits for explaining umbral change involved in long-term evolution but is weak in explaining the flare and flare-related penumbral change. The reconnection scenario proposed by Liu et al. (2005) can successfully explain the flare-related penumbral decay, central umbral darkening, and associated CME. However, this model is weak in explaining the accompanied filament eruption. Besides these two models that could be used to explain this event, let us discuss the classical Kopp-Pneuman model (Kopp & Pneuman 1976), in which the overlying coronal fields are torn open by the dark filament and reconnection of field lines happens subsequently, which eventually restore the pre-flare magnetic configuration. This model has been successful in explaining two-ribbon flares, filament eruption, and the associate CME. However, it hardly can explain the change of magnetic field configuration after flare, as the photospheric magnetic structure is finally

restored to pre-flare configuration. Another well-known standard picture for flare/filament eruptions is the so-called “tether-cutting” model (Sturrock 1989; Moore & Roumeliotis 1992), which involves only a single sheared magnetic arcade in bipolar regions that have a single neutral line on the photosphere where the vertical field component changes sign. However, this model cannot explain CME very well since there is no observational proof of non-anchored bubble-like CME predicted by this model and tether-cutting eruption has not been directly observed in any of the simulations so far. Finally, we turn to the newly-developed model for CMEs and eruptive flares—“magnetic breakout” model. This model not only can explain the flare event accompanied by filament eruption and CME, but also naturally includes the decaying of penumbrae by changing the orientation of field lines from inclined to more vertical configuration. The resulting opened field lines also account for the central umbral darkening. Considering the following critical observational factors for this event: (1) multipolar complex δ configuration plays a crucial role, (2) can explain accompanied filament eruption, (3) can explain accompanied CME, (4) can make magnetic field turn from more inclined to more vertical after magnetic reconnection, we summarize the above five models in table 1.

In this section, we discuss in detail the explanation of the flare-related change in photospheric magnetic field topology in terms of the magnetic breakout model: In the multipolar topology of active region NOAA 9026, reconnection between a sheared arcade and neighboring flux systems removes the unsheared field above the low-lying, sheared core flux near the neutral line, thereby allowing this core flux to burst open and triggering the flare, associated filament eruption, and subsequent CME. The magnetic arcades turn from low-lying to high-lying after the flare due to magnetic reconnection, which causes magnetic fields in the photosphere turn from more inclined to more vertical after the flare.

Panels (a) and (c) of Figure 6 show the cartoons of magnetic field state before the X2.3 flare. The magnetic polarity regions of the δ -spot have a symmetric structure with the symmetry axis along the central neutral line. Two main opposite polarity kernels (the δ -sunspot) are located close to the central neutral line. Two minority opposite polarity footpoints (A4 and A5) are located beside these kernels. For simplicity, we have neglected the effect of peripheral magnetic features. Therefore, we have three photospheric neutral lines and four distinct flux systems: a central arcade that connects the two kernels straddling the middle neutral line (blue field lines), two arcades associated with the bilateral neutral lines connecting each kernel with its opposite polarity footpoint (green field lines), and a flux system that connects the bilateral footpoints (A4 and A5) overlying the three arcades (orange field lines). Note that there are two separatrix surfaces that define the boundaries between the various flux systems and a null point (yellow dot) above the middle neutral line at the intersection of the separatrices. The bilateral (green) arcades are low-lying due

to the confinement of the overlying (orange) arcade which has a tendency to hold down all the arcades below it. Therefore, magnetic field lines are very inclined in regions A1 and A2, which forms the peripheral penumbrae.

As a result of large shear concentrated at the middle neutral line, which may be due to photospheric flows or emergence of new flux, rapid opening and reconnection of/between the central (blue) and the outermost overlying (orange) field lines occur at the null point when the flux systems reach their crucial condition. The breakout of the innermost flux of the central arcade cause the X2.3 flare, 11-degree long filament eruption, and full-halo CME. Figure 6 panels (b) and (d) show the magnetic field state after the X2.3 flare. Due to the opening and reconnection of the low-lying and overlying arcades, some flux is transferred from central (blue) and overlying (orange) systems to the bilateral (green) arcades, and the overlying (orange) arcade that tends to hold down all the other arcades is removed. Due to the removal of holding down tendency, the bilateral (green) arcades become high-lying, which causes the magnetic field lines in the peripheral penumbrae (A1 and A2) turn to be more vertical and turn toward the central umbrae (A3) after the flare. Once the inclination angle (the angle between magnetic field lines and the local horizon) is larger than 45° , Evershed flow will cease, the continuum-intensity signature of which is the disappearance of the associated penumbrae (Leka and Skumanich 1998). Moreover, the magnetic flux in the peripheral penumbrae will decrease when many of magnetic field lines move out of their regions due to the increase of the inclination angle. On the other hand, the magnetic flux in the central umbrae will increase since many field lines move from peripheral penumbral regions into their region. However, we only see a small flux increase instead of expected big increase in A3 from Figure 5. It may be due to Zeeman saturation of filter-based magnetograph in strong umbral fields. But we can clearly see the central umbrae become darker in continuum-intensity from Figure 4 due to the strengthening of their magnetic field.

The authors sincerely thank the referee for valuable suggestions and comments, which helped us to improve the paper significantly. This work was supported by NSF under grant ATM 03-42560, ATM 03-13591, ATM 02-36945, and MRI AST 00-79482 and by NASA under grant NAG 5-13661.

REFERENCES

- Ambastha, A., Hagyard, M.J., & West, E.A. 1993, *Sol. Phys.*, 148, 277
- Antiochos, S.K., DeVore, C.R., & Klimchuk, J.A. 1999, *ApJ*, 510, 485

- Antiochos, S.K. 1998, ApJ, 502, L181
- Aulanier, G., Deluca, E.E., Antiochos, S. K., McMullen, R.A., & Golub, L. 2000, ApJ, 540, 1126
- Chen, J., Wang, H., Zirin, H., & Ai, G. 1994, Sol. Phys., 154, 261
- Denker, C., & Wang, H. 1998, ApJ, 502, 493
- Denker, C., Johannesson, A., Goode, P. R., Marquette, W., Wang, H., & Zirin, H. 1998, Sol. Phys., 184, 87
- Hagyard, M. J., Start, B.A., & Venkatakrishnan, P. 1999, Sol. Phys.184, 133
- Handy, B. N., & 47 co-authors 1999, Sol. Phys.187, 229
- Kopp, R.A. & Pneuman, G.W. 1976, Sol. Phys., 50, 85
- Kosovichev, A. G., & Zharkova, V. V. 1999, Sol. Phys., 190, 459
- Kosovichev, A. G., & Zharkova, V. V. 2001, ApJ, 550, L105
- Kurokawa, H., Wang, T., & Ishii, T.T. 2002, ApJ, 572, 598
- Leka, K. D., & Skumanich, A. 1998, ApJ, 507, 454
- Liu, C., Deng, N., Liu, Y., Falconer, D., Goode, P.R., Denker, C., & Wang, H. 2005, ApJ, Preprint doi: 10.1086/’427868’
- Lynch, B. J., Antiochos, S. K., MacNeice, P. J., Zurbuchen, T. H., & Fisk, L. A. 2004, ApJ, 617, 589L
- Moore, R. L., & Roumeliotis, G. 1992, Eruptive Solar Flares, ed. Z. Svestka, B. V. Jackson, & M. E. Machado (Berlin: Springer)
- Moore, R. L., Hurford, G. J., Jones, H. P., & Kane, S. R. 1984, ApJ, 276, 379
- Sakurai, T., & Hiei, E. 1995, Adv. Space Res., 17, 91
- Scherrer, P. H., & 11 co-authors 1995, Sol. Phys., 162, 129
- Severny, A. B. 1964, ARA&A, 2, 363
- Spirock, T. J., Yurchychyn, V., & Wang, H. 2002, ApJ, 572, 1072
- Sturrock, P. A. 1989, Sol. Phys., 121, 387

- Wang, H., Liu, C., Deng, Y., Zhang, H. 2005, in preparation
- Wang, H., Liu, C., Qiu, J., Deng, N., Goode, P. R., & Denker, C. 2004, ApJ, 601, L195
- Wang, H., Qiu, J., Jing, J., Spirock, T.J., Yurchyshyn, V., Abramenko, V., Ji, H., & Goode, P.R. 2004, ApJ, 605, 931
- Wang, H., Ji, H., Schmahl, E. J., Qiu, J., Liu, C., & Deng, N. 2002, ApJ, 580, L177
- Wang, H., Spirock, T. J., Qiu, J., Ji, H., Yurchychyn, V., Moon, Y.-J., Denker, C., & Goode, P. R. 2002, ApJ, 576, 497
- Wang, H., Goode, P. R., Denker, C., Guo, Y., Yurchychyn, V., Nitta, N., Gurman, J. B., St. Cyr, C., & Kosovichev, A. G. 2000, ApJ, 536, 971
- Wang, H., Ewell, M. W., Zirin, H., & Ai, G. 1994, ApJ, 424, 436
- Wang, H., Tang, F., Zirin, H., & Ai, G. 1991, ApJ, 380, 382
- Yurchyshyn, V.B., Wang, H., Abramenko, V., Spirock, T.J., & Krucker, S. 2004, ApJ, 605, 546
- Zvereva, A. M., & Severny, A. B. 1970, Izv. Krymskoi Astrofiz. Obs., 41-42, 97

Table 1. Summary of Models and Matching of Observational Constraints.

Model	Multipolarity Plays Crucial Role	Explain Filament Eruption	Explain CME	Magnetic Topology Changes
1	Yes	No	No	Yes
2	Yes	No	Yes	Yes
3	No	Yes	Yes	No
4	No	Yes	No	Yes
5	Yes	Yes	Yes	Yes

Note. — Model 1: Kurokawa, Wang, & Ishii (2002). Model 2: Liu et al. (2005). Model 3: Kopp & Pneuman (1976). Model 4: “Tether-Cutting” model—Sturrock (1989); Moore & Roumeliotis (1992). Model 5: “Magnetic Breakout” model—Antiochos (1998); Antiochos, DeVore, & Klimchuk (1999); Lynch et al. (2004).

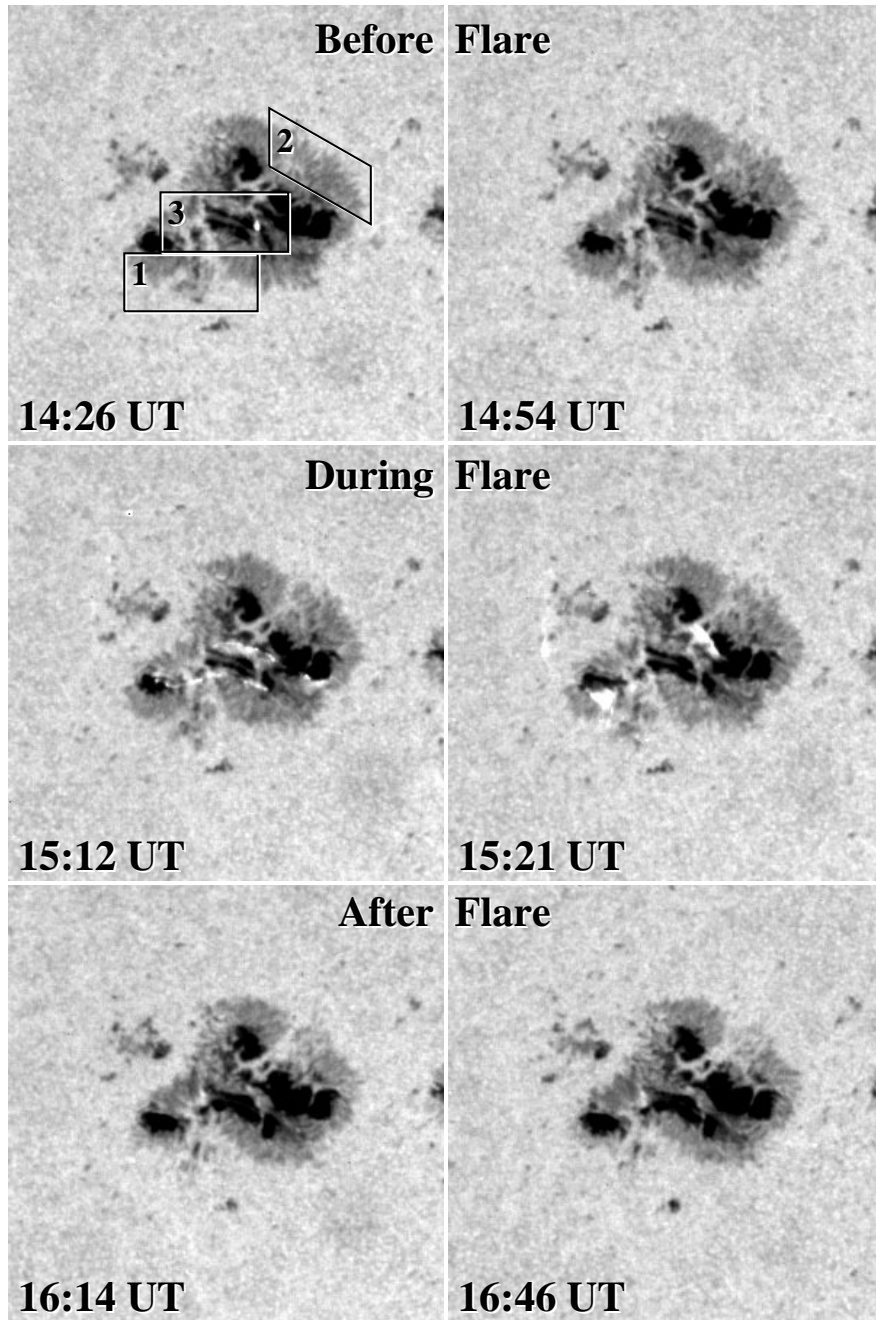


Fig. 1.— Time sequence of TRACE white-light images at 5000 \AA obtained on 2000 June 6 showing the evolution of active region NOAA 9026. Area 1 (A1) and area 2 (A2) outlined by boxes 1 and 2 respectively refer to the two disappearing penumbrae. Area 3 (A3) outlined by box 3 includes the darkening central umbrae. The FOV is $150'' \times 150''$.

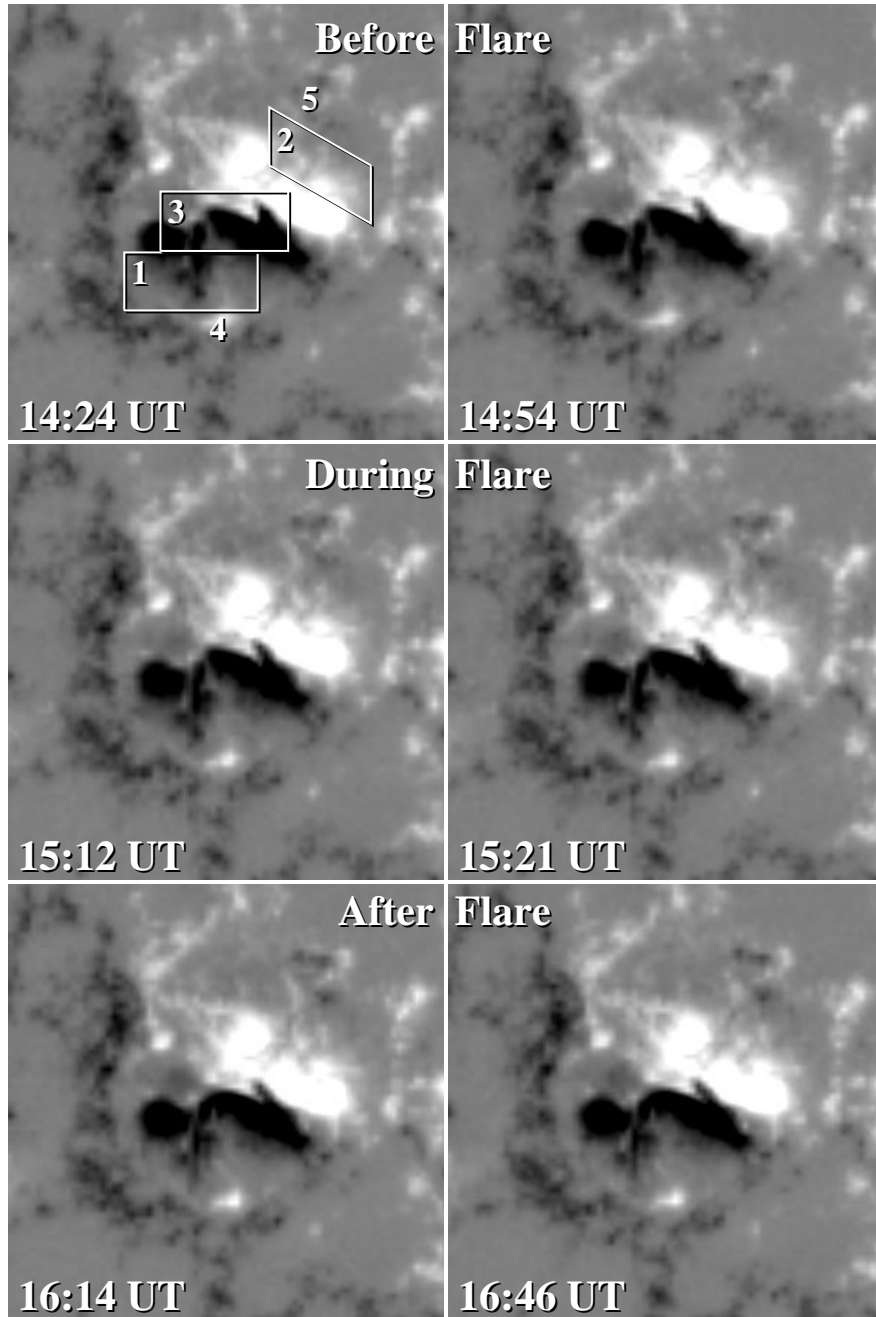


Fig. 2.— Time sequence of MDI line-of-sight magnetograms corresponding to Figure 1. A1, A2, and A3 are the same regions as shown in Figure 1. 4 and 5 denote the localized emerging/strengthening opposite polarity regions around the δ -sunspot.

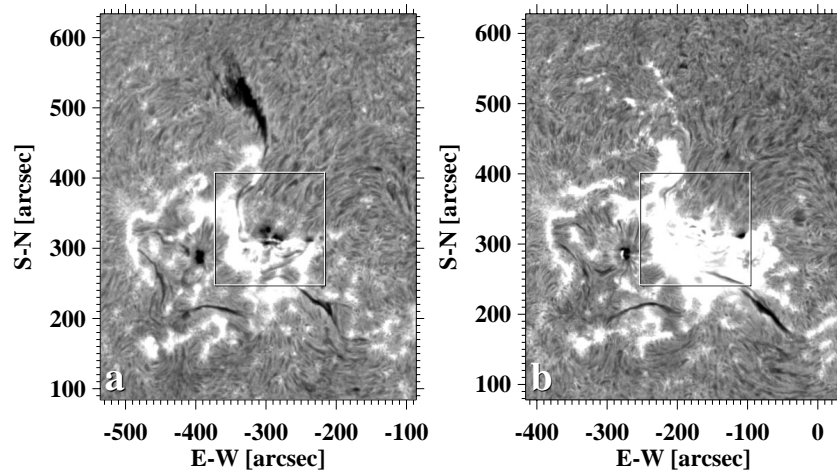


Fig. 3.— Detailed view of BBSO full disk $H\alpha$ images (a) on 2000 June 5 at 23:28:46 UT before and (b) on 2000 June 6 at 16:14:21 UT after the flare showing the location of the 11-degree long filament eruption. The filament was essentially located on the neutral line of the δ -spot before the flare. The region indicated by the box is the same FOV as shown in Figures 1 and 2.

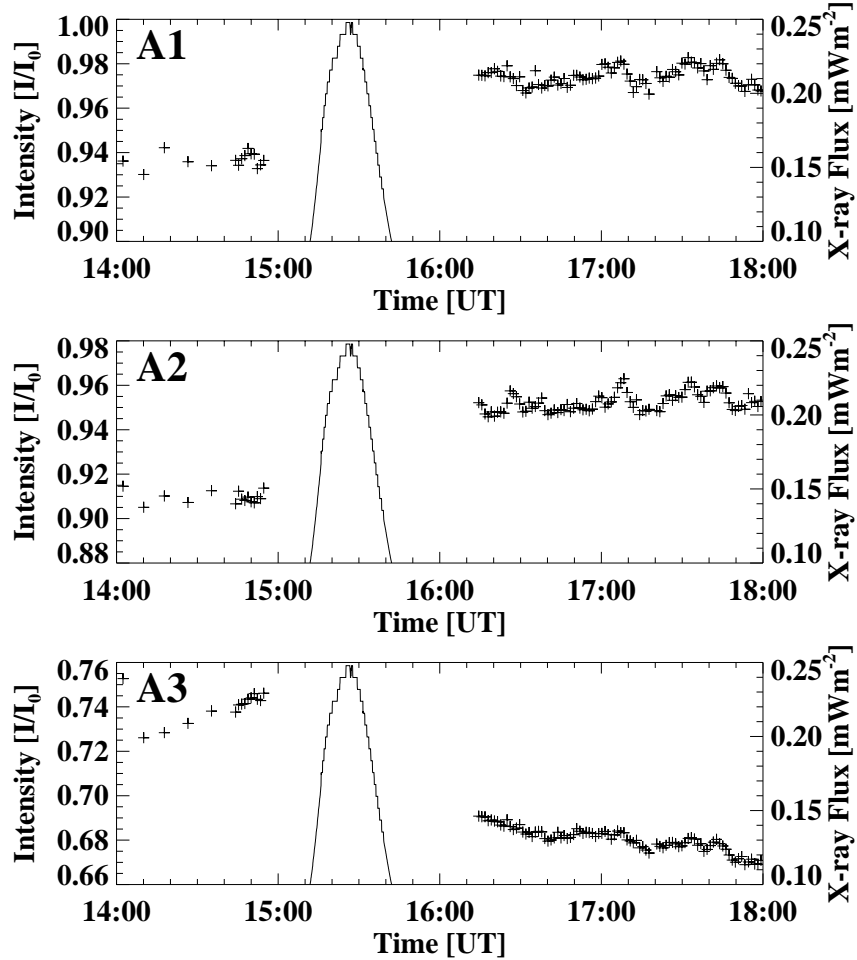


Fig. 4.— Temporal evolution of the average intensity from TRACE white-light images in areas A1, A2, and A3 (plus signs). The GOES X-ray flux in the 1 Å to 8 Å band is depicted in each panel with solid line to illustrate the X2.3 flare. The data gap between 14:54 UT and 16:14 UT results from eliminating the data during the flare when bright flare ribbons traverse areas A1, A2, and A3.

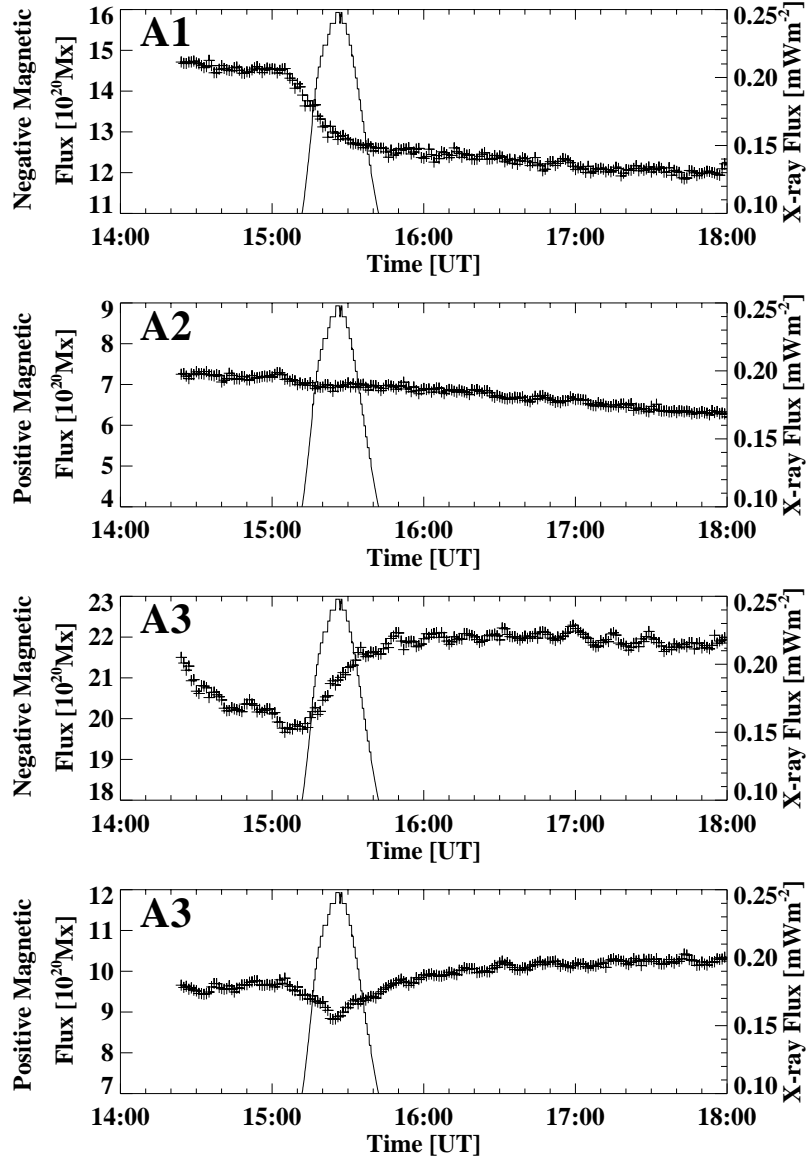


Fig. 5.— Temporal evolution of the average magnetic flux from MDI line-of-sight magnetograms in areas A1, A2, and A3 (plus signs). The GOES X-ray flux in the 1 Å to 8 Å band is depicted in each panel with solid line to illustrate the X2.3 flare.

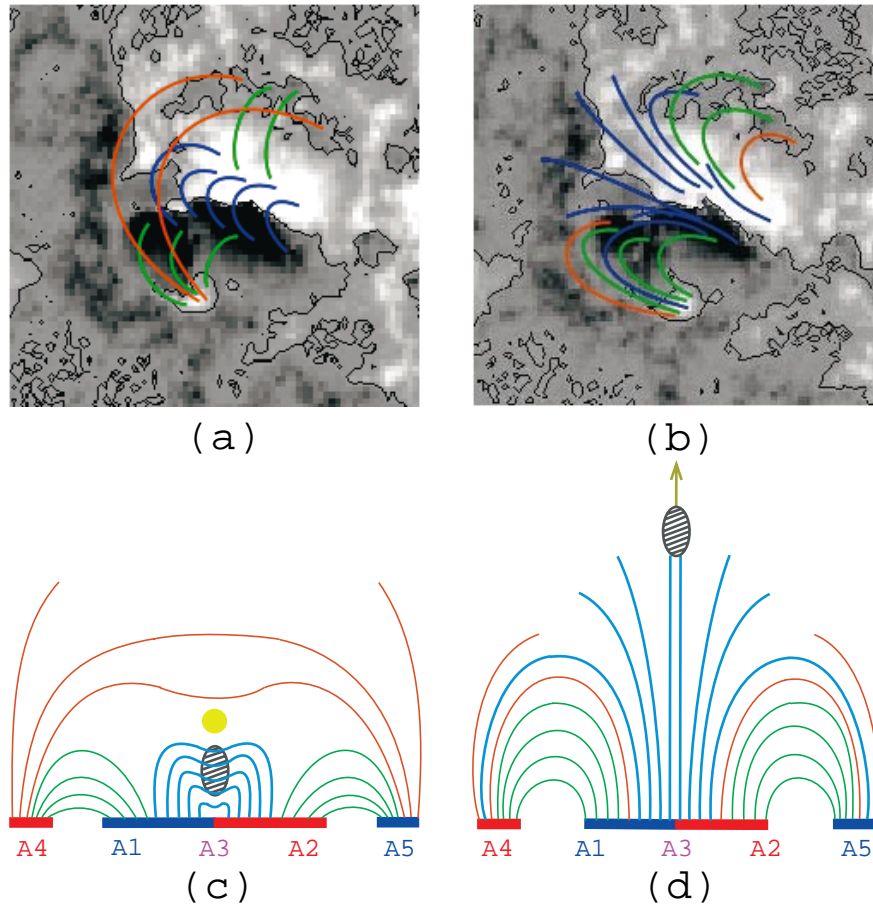


Fig. 6.— (a) MDI line-of-sight magnetogram with neutral line before the X2.3 flare, the colored lines are a cartoon of the magnetic field topology before flare; (b) MDI line-of-sight magnetogram with neutral line after the X2.3 flare, the colored lines are a cartoon of the magnetic field topology after flare; (c) two-dimensional scheme of magnetic field lines before the X2.3 flare; (d) two-dimensional scheme of magnetic field lines after the X2.3 flare. The magnetic topology is based on the magnetic breakout model.